Research in Astronomy and Astrophysics, 24:015001 (7pp), 2024 January https://doi.org/10.1088/1674-4527/ad089e

Formation of a Rapidly Rotating Classical Be-star in a Massive Close Binary System

Evgeny Staritsin
K.A. Barkhatova Kourovka Astronomical Observatory, B.N. Yeltsin Ural Federal University, pr. Lenina 51, Ekaterinburg 620000, Russia; Evgeny.Staritsin@urfu.ru
Received 2023 July 3; revised 2023 October 23; accepted 2023 October 27; published 2023 December 12

Abstract

This paper investigates the spin-up of a mass-accreting star in a close binary system passing through the first stage of mass exchange in the Hertzsprung gap. Inside an accreting star, angular momentum is carried by meridional circulation and shear turbulence. The circulation carries part of the angular momentum of the accreted layers to the accretor's surface. The greater the rate of arrival of angular momentum in the accretor is, the greater this part. It is assumed that this part of the angular momentum can be removed by the disk further from the accretor. If the angular momentum in the matter entering the accretor is more than half the Keplerian value, then the angular momentum obtained by the accretor during mass exchange stage does not depend on the rate of arrival of angular momentum. The accretor may have the characteristics of a Be-star immediately after the end of mass exchange.

Key words: (stars:) binaries (including multiple): close – stars: emission-line – Be – stars: early-type – stars: rotation

1. Introduction

Classical Be-stars include OBA stars with observed or previously observed emissions in the Balmer lines of hydrogen (Porter & Rivinius 2003). These stars are not supergiants and have large rotational velocities. Among Be-stars, there is the group of early spectral subclasses (B3–O9). The surface rotational velocities of these stars range widely. The lower range limit is 40%–60% of the Keplerian value, while the upper limit is 90%–100% (Cranmer 2005). The origin of the large rotational velocities of Be-stars is not clear.

Young B-stars in the early spectral subclasses and O-stars are characterized by lower rotational velocities (Huang et al. 2010); 70% of these stars are observed in binary and multiple systems (Chini et al. 2012; Sana et al. 2012). All these stars are expected to form binary and multiple systems, considering selection effects. Mass exchange in a binary system may be the reason for the rapid rotation of the star receiving mass. The synthesis of the Be-star population in binary systems makes it possible to reproduce the observed number of these stars in the Galaxy (Pols et al. 1991; Portegies Zwart 1995; Van Bever & Vanbeveren 1997; Shao & Li 2014; Hastings et al. 2021).

A simple estimation made assuming the instantaneous redistribution of angular momentum in the stellar interior to solid-state rotation shows that a 5%–10% increase to the star's mass due to accretion of mass with Keplerian velocity leads to a critical rotation state (Packet 1981). The question of what happens when there is continued accretion into a star close to a state of critical rotation has been discussed in Paczyński (1991), Popham & Narayan (1991), Colpi et al. (1991), and Bisnovatyi-Kogan (1993). Paczyński (1991), Popham & Narayan (1991), and Colpi et al. (1991) used various approaches. All authors agree that accretion does not stop when the star's speed of rotation reaches a critical value. Paczyński (1991) studied the whole star-boundary layer-accretion disk system for various rotations of the central star. For models rotating slightly above critical, mass accretion is accompanied by the loss of angular momentum from the star to the disk, mediated by viscous stresses. However, the solutions obtained in Paczyński (1991), Popham & Narayan (1991), and Colpi et al. (1991) are not self-consistent. The condition for a self-consistent solution for a system consisting of a star in a state of critical rotation and an accretion disk is that "the star absorbs accreted matter with a certain angular momentum, such that the star remains in a state of critical rotation" (Bisnovatyi-Kogan 1993). Let $J(M)$ be the angular momentum of a star with mass M in a state of critical rotation and let $j_e^{\rm Kep}$ be the specific Keplerian angular momentum at the equator of the star. Then $j_a = dJ/dM < j_e^{\rm Kep}$. A mass-accreting star can move along the sequence of stars in a state of critical rotation $J(M)$ if the excess angular momentum of $\triangle j = j_e^{\rm Kep} - j_a$ is eliminated. Bisnovatyi-Kogan (1993) constructed models of accretion disks that remove excess angular momentum from the surface of a star. At the same time, the speed of rotation at the star's surface remains critical. So, an increase in the mass and angular momentum of a star in a critical rotation state may occur due to the removal of excess angular momentum from the star by the accretion disk (Paczyński 1991; Bisnovatyi-Kogan 1993).

Physical processes, such as meridional circulation and turbulence, require finite amounts of time to transfer angular

momentum (Staritsin 2019, 2021). At the very beginning of accretion, only the outer layers of the star, including the accreted mass, have a fast rotation. The star surface gains critical rotation shortly after the start of accretion. Later, at the accretion stage in a state of accretor critical rotation, the circulation carries part of the angular momentum brought along with the accreted mass from subsurface layers to the star's surface (Staritsin 2022). Thus, accreted layers can shrink, as usually happens during accretion. The angular momentum transferred by circulation to the star's surface can be removed through an accretion disk (Paczyński 1991; Bisnovatyi-Kogan 1993). Thus, the mass and angular momentum of an accretor in a state of critical rotation increase due to the removal of excess angular momentum from the accreted layers to the accretor surface and the further removal of this angular momentum from the star.

In Staritsin (2022), the transfer of angular momentum in the accretor interior was carried out only by meridional circulation. The turbulence was artificially suppressed. This made it possible to elucidate the transport properties of circulation in an accreting star's interior. The role of turbulence in angular momentum transport within the accretor remained unclear. As to the angular momentum input, only one option has been considered, the effective transport of angular momentum from the disk's boundary layer to the accretor's upper layer.

In this paper, we consider two mechanisms of angular momentum transfer in an accreting star interior, namely circulation and turbulence. This allows us to find the role of turbulence in the spinning up of a star. We also take into account the possible reduction of input angular momentum. This decrease can be attributed both to the transfer of angular momentum from the boundary layer to the outer parts of the disk, and to sub-Keplerian rotation in the disk. The accretor's rotation, obtained as a result of mass exchange, has been studied depending on the angular momentum introduced during mass exchange.

2. Basic Equations and Simplifications

2.1. The Angular Momentum Input

The matter lost by the donor due to the filling of the Roche lobe falls into the accretor's gravitational field and swirls around it. The formation of gas structures around the accretor, in particular the formation of a disk and a velocity field in it, depends on the ratio between three factors: the size of the accretor R, the minimum distance $\omega_{\min}$ from the center of the accretor to the central line of the stream of matter falling from donor point L_1, and the distance from the accretor's center to the edge of the inviscid disk ω_d (Lubow & Shu 1975).

Transient disks with sub-Keplerian rotation have been found (for example, RW Tau (Kaitchuck & Honeycutt 1982) and β Per (Cugier & Molaro 1984; Richards 1992)) in direct-impact systems ($\omega_d < R$). Three-dimensional hydrodynamic calculations show disk formation in such systems; the rotation velocity is 80% and 60% of the Keplerian value at the inner and outer edges of the disk, respectively (Raymer 2012).

Both transient disks (SW Cyg) and permanent, but variable, accretion disks (RY Gem, TT Hya, AU Mon) in grazing-impact systems ($\omega_{\min} < R < \omega_d$) have been discovered. The velocity fields in the transient disk of the SW Cyg system and in the permanent disk of the RY Gem system are sub-Keplerian (Kaitchuck 1988, 1989). Asymmetric parts were found in the disks of the TT Hya and AU Mon systems; the gas in the disk's asymmetric part in the AU Mon system moves at a sub-Keplerian velocity (Richards et al. 2014). Hydrodynamic calculations also show the possibility of disk formation at sub-Keplerian velocities in these systems (Richards & Ratliff 1998).

Permanent disks are found in systems with $R < \omega_{\min}$. The radial component of the matter velocity in the disk is directed toward the accretor and is 10–30 km s^{-1}. The change in the tangential component with distance from the accretor may differ from the Keplerian one (Etzel et al. 1995).

The aforementioned observational data and the results of hydrodynamic calculations relate to systems with the low mass of accreting components ($M \leqslant 6\,M_{\odot}$) and with a ratio of donor mass to accretor mass within the range of 0.2–0.3. The formation of Be-stars in the early spectral subclass occurs in systems with large component masses. The ratio of donor mass to accretor mass varies widely. Mass transfer in such systems is non-conservative (Van Rensbergen et al. 2011; Deschamps et al. 2015). The star receiving mass increases in volume (Benson 1970; Kippenhahn & Meyer-Hofmeister 1977). The distance between two stars depends on how the system loses mass and angular momentum. So, the formation of gas structures in the Roche lobe of an accretor depends on the loss of mass and angular momentum from the system. A quantitative theory of mass and angular momentum losses from a close binary system has not yet been developed. The formation of conditions for sub-Keplerian rotation in an accretion disk due to the loss of mass and angular momentum from the binary system cannot be ruled out. Thus, the possibility of mass accretion with sub-Keplerian velocities of rotation should be considered.

At the very beginning of accretion, when accretor rotation velocity is low, the rotation velocity of disk matter decreases in the narrow boundary layer from the maximum value in the disk $\Omega_{\max}$ to the value on the star's surface Ω_s (Paczyński 1991). Turbulence can remove angular momentum from the boundary layer to an accretor's upper layers at a rate of

$$\frac{dJ}{dt} = \frac{2}{3}R^2(\Omega_{\max} - \Omega_s)\dot{M}, \tag{1}$$

where J—angular momentum of the accretor, t—time, and $\dot{M}$—mass accretion rate.

Supersonic shear flow in the boundary layer is a source of acoustic waves. The waves can carry the angular momentum out of the boundary layer both into the accretor's outer part and the disk's outer part (Dittmann 2021; Coleman et al. 2022). In this case, the amount of angular momentum coming from the boundary layer into the accretor is less than the Keplerian one.

In an earlier study (Staritsin 2022), we considered the following: when at the stage of subcritical rotation, angular momentum enters the accretor through two channels, namely together with matter having the same rotation velocity as the accretor's surface and due to turbulence within the rate (1). This is a case of high efficiency of angular momentum transfer from the boundary layer to the accretor's upper part. The transfer of angular momentum in the accretor's interior was carried out by meridional circulation; turbulence was artificially suppressed.

In the current calculations, angular momentum transfer in the accretor's interior can be carried out both by meridional circulation and turbulence. We have studied two variants for the arrival of angular momentum into the accretor.

In the first variant, to clarify the influence of angular momentum transport by turbulence in the accretor's interior on the spinning up of the accretor, we calculated accretion with the same rate of arrival of angular momentum into the accretor as in Staritsin (2022). At the stage of subcritical rotation, the parameter $\Omega_{\max}$ in the angular momentum source (1) is equal to $\alpha\,\Omega^{\rm Kep}$, where $\alpha = 0.8$; here, $\Omega^{\rm Kep}$ is the Keplerian velocity of the star's surface at the equator. After the angular velocity of the accretor's surface increases to the $\alpha\,\Omega^{\rm Kep}$ value, the arrival of angular momentum from the boundary layer (1) stops. The angular velocity of the added matter is set equal to $\alpha\,\Omega^{\rm Kep}$ for the remainder of the mass exchange.

In the second variant, the case of extremely low efficiency of angular momentum transfer from the boundary layer to the accretor's upper part is considered. The angular momentum's source (1) in this case is assumed to be zero. As long as the angular velocity of the star's surface is less than $\alpha\,\Omega^{\rm Kep}$, the star accretes matter with the same angular velocity as that of the star's surface. After the surface angular velocity increases to the value of $\alpha\,\Omega^{\rm Kep}$, the angular velocity of the added matter remains equal to $\alpha\,\Omega^{\rm Kep}$. In order to determine the dependence of the accretor's rotation state after the end of mass exchange on the content of angular momentum in adding mass, calculations were carried out at four values of α: 0.8, 0.6, 0.4, and 0.2.

2.2. Angular Momentum Transfer in the Accretor's Interior

Angular momentum transfer in the radiative layers of a star is taken into account in the framework of the shellular rotation model (Zahn 1992). In terms of this model, two mechanisms of angular momentum transfer are considered: meridional circulation and shear turbulence. The angular momentum transfer is described by the law of conservation of angular momentum (Tassoul 1978)

$$\frac{\partial(\rho\varpi^2\Omega)}{\partial t} + \mathrm{div}(\rho\varpi^2\Omega\boldsymbol{u}) = \mathrm{div}(\rho\nu_{\rm v}\varpi^2\,\mathrm{grad}\Omega).$$

The meridional circulation velocity $\boldsymbol{u}$ is determined from the law of conservation of energy in a stationary form (Maeder & Zahn 1998)

$$\rho T\boldsymbol{u}\,\mathrm{grad}s = \rho\varepsilon_n + \mathrm{div}(\chi\,\mathrm{grad}T) - \mathrm{div}\boldsymbol{F}_h.$$

In these equations, ρ—density, ϖ—distance to the axis of rotation, Ω—angular velocity, $\nu_{\rm v}$—turbulent viscosity in the vertical direction, T—temperature, s—specific entropy, ε_n—nuclear energy release rate, χ—thermal conductivity, $\boldsymbol{F}_h$—turbulent enthalpy flow in the horizontal direction: $\boldsymbol{F}_h = -\nu_h\rho T\partial s/\partial\boldsymbol{i}_\theta$ with ν_h turbulent viscosity in the horizontal direction. The coefficients of turbulent viscosity were determined by Talon & Zahn (1997), Maeder (2003), and Mathis et al. (2004). The convective core rotates in a solid-state manner. These equations are solved together with equations related to the structure and evolution of stars. We used a set of programs from Paczyński (1970) modified to calculate the evolution of rotating stars (Staritsin 1999, 2005, 2007, 2009, 2014).

3. Calculation Results

3.1. Binary System Parameters

We consider mass exchange in a binary system with the component masses of 13.4 and 10.7 $M_\odot$ and the period $P = 35^d$ as in Staritsin (2022). By the beginning of mass exchange, star rotation with a mass of 10.7 $M_\odot$ is synchronized with orbital motion. The star's angular momentum is equal to $1.3\times10^{51}\,\mathrm{g\cdot cm^2\,s^{-1}}$. A star with a mass of 13.4 $M_\odot$ loses 10.5 $M_\odot$ in 12,000 yr. After that, the star decouples its Roche lobe and the mass exchange stage ceases.

The second star accretes 5.3 $M_\odot$. The final mass of the accretor is 16.0 $M_\odot$. The accretion rate was set constant, equal to the average value of $\sim4.4\times10^{-4}\,M_\odot\,\mathrm{yr}^{-1}$. We consider a case when the entropy of the added matter is the same as the surface layers of the second star. The thermal timescale of the second star is longer than mass exchange duration. The star's reaction to the increase in mass in this case is well understood (Benson 1970; Flannery & Ulrich 1977; Neo et al. 1977). The second star is driven out of thermal equilibrium by mass accretion. Nuclear power output in the center of the second star increases, and some of the nuclear energy release is spent on an increase in entropy in the second star's central parts. Gravitational energy release in the surface layers is added to nuclear energy release in the center. The typical luminosity distribution in the second star's interior is shown in (Staritsin 2022) (see their Figure 4).

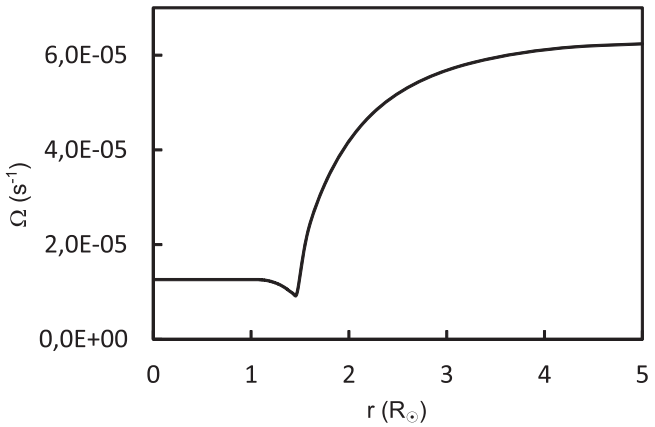

Figure 1. Angular velocity at the bottom of the outer cell of the meridional circulation at the beginning of mass exchange.

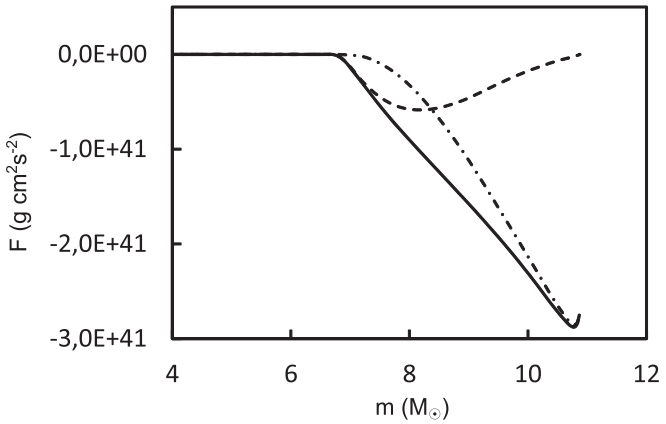

Figure 2. Turbulent (dashed-line), advective (dot-dashed line), and total (solid line) angular momentum flux in the accretor's interior at the stage of subcritical rotation.

The remaining part of the mass lost by the first star leaves the system. The tidal interaction between the two stars is unable to synchronize the accreting star with the orbit due to the long period of the system and the short accretion timescale. The accretion of matter and angular momentum, as well as transport processes inside the accretor and in the disk, determines the accretor's angular momentum.

3.2. The Case of the High Efficiency of Angular Momentum Transfer from the Boundary Layer to the Accretor's Upper Part

With the beginning of mass exchange, a circulation cell is formed in the subsurface layer of the accretor, in which the circulation carries the incoming angular momentum downwards. The cell consists of accreted layers and the swirled layers of the accretor located below. In the cell's upper part, angular velocity has an almost constant value, but near the bottom of the cell, it sharply reduces to the initial value (Figure 1). Therefore, in the lower part of the cell, the contribution of turbulence to angular momentum transfer is greater and exceeds the contribution of meridional circulation (Figure 2). The bottom of the cell goes down into the star faster than when turbulence is artificially suppressed. The angular momentum entering the accretor is distributed over a larger mass of matter than in the case of suppressed turbulence. The rotation of the accretor's surface becomes critical when its mass increases to 11.3 $M_\odot$ (in the case of suppressed turbulence—up to 11.0 $M_\odot$ (Staritsin 2022)). The distribution of angular velocity in the accretor's interior at this moment is shown in Figure 3.

At the stage of critical rotation, the mass of the accretor increases by another 4.7 $M_\odot$. Another circulation cell is formed in the accreted matter. In this cell, the circulation transfers the sum part of the angular momentum that came along with the

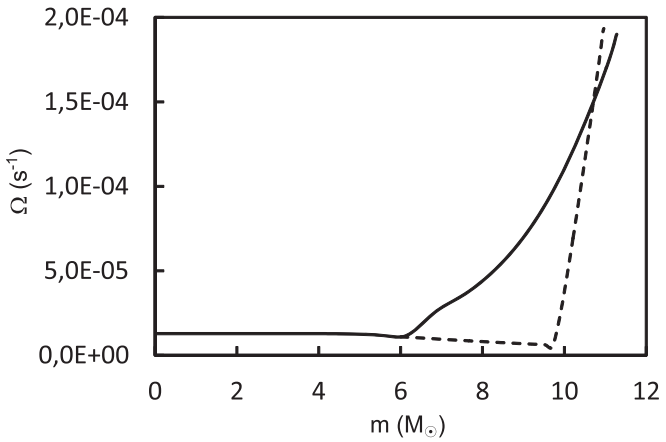

Figure 3. Angular velocity when the rotation of the accretor's surface becomes critical and when active turbulence (solid line) and artificially suppressed turbulence are present (Staritsin 2022) (dashed line).

accreted mass to the surface of the accretor (Figure 4). It is assumed that this part of the angular momentum is removed from the accretor by the accretion disk (Paczyński 1991; Bisnovatyi-Kogan 1993). As a result of a decrease in angular momentum, the accreted layers are contracted. The velocity of their rotation is permanently lower than the Keplerian velocity.

In the circulation cell formed at the beginning of mass exchange, the transfer of angular momentum inside the accretor continues. The mass of the matter in this cell increases as the upper boundary of the cell moves up along the accretor mass, and the bottom of the cell moves down. The bottom of the cell goes down to the convective core when the accretor mass increases to 11.9 $M_\odot$ (in the case of suppressed turbulence—up to 15 $M_\odot$ (Staritsin 2022)). The role of turbulence lies in the rapid lowering of the bottom of the circulation cell, in which

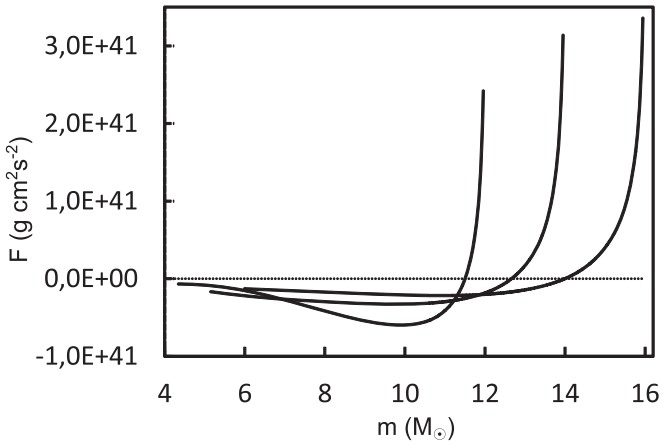

Figure 4. Angular momentum flux in the accretor's interior when its mass is equal to 12, 14, and 16 $M_{\odot}$.

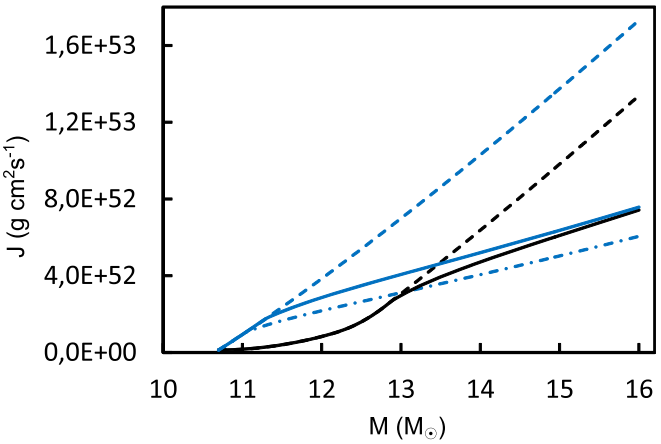

Figure 5. The angular momentum amount entering the accretor (dashed lines), the angular momentum of the accretor (solid lines) depending on its mass at $\alpha = 0.8$ when the source of the angular momentum (1) is considered (blue color) and is not taken into account (black color). The case of artificially suppressed turbulence (Staritsin 2022) is also shown (dot-dashed line).

the circulation carries angular momentum into the star's interior.

The amount of angular momentum removed from the accretor during mass exchange depends slightly on processes of angular momentum transfer within the accretor (Figure 5). When turbulence is present, the amount of angular momentum transferred to the accretor's inner layers increases, and the amount of angular momentum carried to the accretor's surface decreases compared to the case of suppressed turbulence (Table 1). The angular momentum brought into the accretor during mass exchange is $1.72 \times 10^{53}\,\mathrm{g \cdot cm^2\,s^{-1}}$; 12% of this value enters the inner layers that made up the accretor initially, 31% remains in the accreted mass, and 57% is carried to the accretor's surface and is removed by the disk. In the case of suppressed turbulence, the corresponding values are 5%, 30%, and 65% (Staritsin 2022). After the end of mass exchange, the accretor's angular momentum is greater when turbulence is present (Table 1).

Table 1
Angular Momentum Balance

No	Case 1	Case 2	Case 3	Case 4	Case 5	Case 6
J_1	17.2	17.2	13.3	10.3	6.9	3.7
J_2	11.2	9.7	6.0	3.0	0.0	0.0
J_3	5.2	5.4	5.3	5.3	5.1	2.9
J_4	0.8	2.1	2.0	2.0	1.8	0.8
J_5	6.1	7.6	7.4	7.4	7.0	3.8

Note. The rows show as follows: (J_1) the angular momentum that entered the accretor during mass exchange; (J_2) the angular momentum removed from the accretor during mass exchange; (J_3) the angular momentum remaining in the accreted mass; (J_4) the angular momentum transferred to the part of the accretor that made up the star initially; (J_5) the angular momentum of the accretor after mass exchange, the angular momentum is expressed in units of $10^{52}\,\mathrm{g \cdot cm^2\,s^{-1}}$. The columns show the results for the following cases: (Case 1) angular momentum transfer from the boundary layer is considered, turbulence in the accretor's interior is artificially suppressed (Staritsin 2022); (Case 2) angular momentum transfer from the boundary layer is considered, turbulence in the accretor interior is considered; (Case 3), (Case 4), (Case 5), and (Case 6) angular momentum transfer from the boundary layer is not considered, turbulence in the accretor interior is present, and α is equal to 0.8, 0.6, 0.4, and 0.2, respectively.

3.3. The Case of Extremely Low Efficiency of Angular Momentum Transfer from the Boundary Layer to the Accretor's Upper Part

At the beginning of mass exchange, the rotation velocities of the incoming mass and the accretor's surface coincide. The rate of angular momentum arrival into the accretor is significantly less than when turbulence and/or waves transfer angular momentum from the boundary layer to the accretor's outer part. Due to the low rate at which angular momentum enters the accretor, the accretor's angular momentum increases slowly at the beginning of accretion (Figure 5).

The general picture of angular momentum transfer in the accretor's interior at α equal to 0.8 and 0.6 is the same as when angular momentum goes from the boundary layer to the accretor's upper part. The difference is that the total amount of angular momentum that has entered the accretor during mass exchange decreases (Table 1). Reasons for the decrease are associated with the absence of a source (1) and a decrease in parameter α. However, with α equal to 0.8 and 0.6, the accretor surface's rotation velocity increases to a critical value. This occurs when accretor mass increases to 12.9 and 13.3 $M_{\odot}$, respectively (Figure 6). In these cases, a circulation cell is formed in the accretor's outer layer, in which the circulation transfers part of the angular momentum of the accreted layers to the accretor's surface. The amount of angular momentum

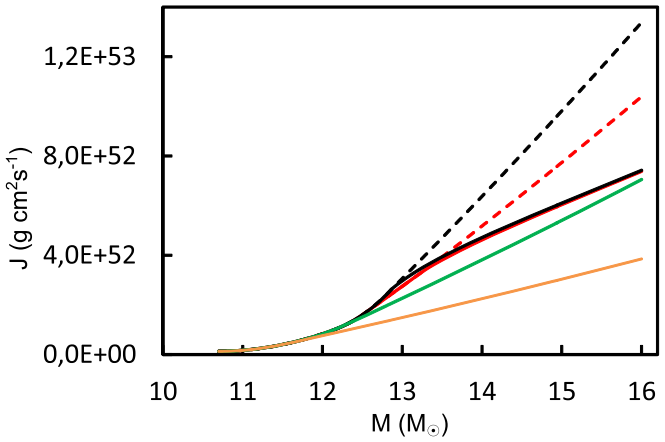

Figure 6. The angular momentum amount entering the accretor (dashed lines), the angular momentum of the accretor (solid lines) depending on its mass at $\alpha = 0.8$ (black), $\alpha = 0.6$ (red), $\alpha = 0.4$ (green), and $\alpha = 0.2$ (orange) when the source of angular momentum (1) is not considered. At $\alpha = 0.4$ and $\alpha = 0.2$, the accretor retains the entire angular momentum obtained with the accreted mass, so the dashed lines coincide with the solid ones.

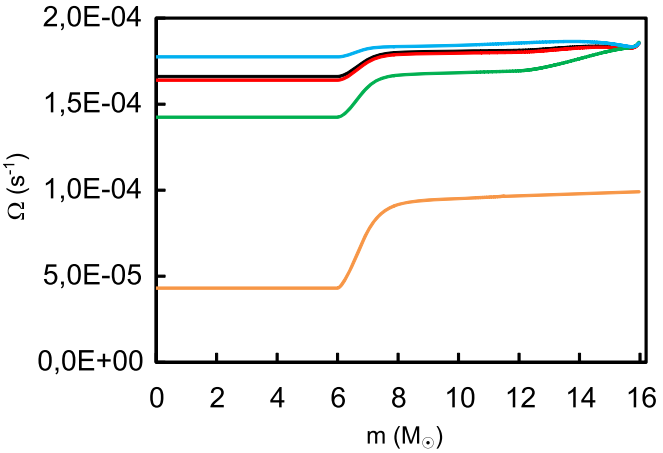

Figure 7. The distribution of angular velocity in the accretor's interior after the end of mass exchange in cases when the source of angular momentum (1) is considered (blue) and not considered at $\alpha = 0.8$ (black), $\alpha = 0.6$ (red), $\alpha = 0.4$ (green), and $\alpha = 0.2$ (orange).

removed from the accreted layers and lost by the accretor in these cases is less than in calculations with a source (1) (Table 1). The state of accretor rotation once mass exchange finishes is approximately the same as when the angular momentum's arrival from the boundary layer to the accretor's upper part was considered. A decrease in angular momentum entering the accretor only results in decreases in the angular momentum taken out of the accretor at the stage of accretion during accretor critical rotation.

At α equal to 0.4 and 0.2, a smaller amount of angular momentum enters the accretor (Table 1). The rotation velocity of the accretor's surface remains subcritical throughout the entire mass exchange stage; at α equal to 0.4, it approaches the critical value by the end of this stage. In both cases, at the beginning of mass exchange, a circulation cell is formed in the accretor's subsurface layer, in which the angular momentum of the accreted matter is transferred inside the accretor. The bottom of the cell goes down to the convective core when the mass of the accretor increases to 13.1 $M_\odot$ at α equal to 0.4 and up to 13.9 $M_\odot$ at α equal to 0.2. In both cases, the angular momentum of the accreted mass is transferred inside the star throughout the mass exchange stage. The accretor retains all the angular momentum received with the accreted mass (Figure 6). Once mass exchange finishes, the angular momentum of the accretor at α equal to 0.4 is a little less than at α equal to 0.6 and 0.8, and at α equal to 0.2 is significantly less (Table 1).

3.4. Accretor Rotation State After Mass Exchange

The distribution of the angular velocity of rotation in the accretor's interior immediately after the end of mass exchange is shown in Figure 7. In all cases, angular velocity decreases rapidly in a layer of variable chemical composition located between the chemically homogeneous part of the radiative envelope and the convective core. A similar jump is formed in cases where angular momentum enters the accretor in a short time—in the donor's thermal timescale or faster (Staritsin 2021). The thermal timescale of the accretor is longer than that of the donor in the cases considered in Staritsin (2021, 2022). After the end of mass exchange, the jump gradually decreases and disappears during the thermal timescale of the accretor (see, for example, Figure 3 in Staritsin 2021).

The angular velocity in the accretor's interior after mass exchange when α is equal to 0.8 and α is equal to 0.6 almost does not depend on what the content of the angular momentum was in the added mass and on whether angular momentum is transferred from the boundary layer to the accretor's upper layer (Figure 7). In these cases, the accretor's angular momentum is almost equal to $\sim 7.5 \times 10^{52}\,\mathrm{g \cdot cm^2\,s^{-1}}$ (Table 1) after the mass exchange. An isolated star with a mass of 16 $M_\odot$ has a critical rotation throughout the stage of hydrogen burning in the core with this angular momentum value (Staritsin 2007). Consequently, due to the exchange of mass, the accretor receives a rotation typical for Be-stars.

At α equal to 0.4, the accretor receives almost the same angular momentum with accreted mass as the angular momentum that remains in the accretor when α is 0.8 and α is 0.6 (Table 1). Therefore, at α equal to 0.4, the accretor also has a rotation typical for Be-stars. At α equal to 0.2, the accreted mass brings a much lower angular momentum (Table 1). The angular velocity in the accretor's interior is lower than in other cases (Figure 7). The rotation of the accretor's surface immediately after mass exchange in this case is lower than that of Be-type stars. In an isolated star with the

same mass and angular momentum as the accretor, the removal of angular momentum from the inner layers to the outside occurs intensively at the stage of hydrogen burning in the core (Staritsin 2007, 2009). The angular velocity of the star's surface, expressed in Keplerian angular velocity, increases; at the last steps of this stage, the star acquires a rotation typical for Be-stars of the early spectral subclass. If tidal interaction is low, then even in this case the accretor can obtain the characteristics of a Be-star after the end of mass exchange, but only after a long period of time on the order of part of the hydrogen burning stage in the core.

4. Conclusions

Meridional circulation is a flexible mechanism for the transfer of angular momentum in the stellar interior of a rotating star. The direction and rate of angular momentum transfer by circulation may vary widely at the stage of mass accretion, depending on the star's rotation state and the rate of angular momentum arrival along with the accreted mass and waves and/or due to turbulence. The two main circulation cells are formed due to the accretion of mass and angular momentum. In the cell, which is formed at the stage of subcritical rotation of the accretor, circulation transfers the angular momentum inside the accretor. Only in the lower part of this cell does turbulence make the main contribution to the transfer of angular momentum. Due to turbulence, the cell bottom quickly goes downwards into the accretor's interior. In a cell formed at the stage of critical rotation, the circulation transfers part of the angular momentum of the accreted mass to the surface of the star; the more the content of the angular momentum in the entering matter is, the greater this part.

We have considered the case of mass exchange in a binary system, when half of the mass lost by the donor falls into the accretor. If the angular momentum of the mass falling into the accretor exceeds half the Keplerian value at the boundary of the accretor, the state of rotation of the accretor after the end of mass exchange does not depend on the angular momentum entering the accretor. In other words, processes that could reduce the angular momentum of the matter located around the accretor to no more than half the Keplerian value do not affect the angular momentum and the state of rotation that the accretor receives by the end of the mass exchange stage. These processes impact the amount of angular momentum removed by circulation from the accreted mass to the accretor's surface and removed further from the accretor by a disk or other processes.

In the considered system with the initial component masses of 13.4 and 10.7 $M_{\odot}$, the accretor has a rotation typical for Be-stars immediately after the end of mass exchange, if during mass exchange the angular momentum of the mass added to the accretor exceeds 40% of the Keplerian value.

Acknowledgments

This work was supported by the Ministry of Science and Education, FEUZ-2023-0019.

References

Benson, R. S. 1970, BAAS, 2, 295
Bisnovatyi-Kogan, G. S. 1993, A&A, 274, 796
Chini, R., Hoffmeister, V. H., Nasseri, A., Stahl, O., & Zinnecker, H. 2012, MNRAS, 424, 1925
Coleman, M. S. B., Rafikov, R. R., & Philippov, A. A. 2022, MNRAS, 512, 2945
Colpi, M., Nannurelli, M., & Calvani, M. 1991, MNRAS, 253, 55
Cranmer, S. R. 2005, ApJ, 634, 585
Cugier, H., & Molaro, P. 1984, A&A, 140, 105
Deschamps, R., Braun, K., Jorissen, A., et al. 2015, A&A, 577, A55
Dittmann, A. J. 2021, MNRAS, 508, 1842
Etzel, P. B., Olson, E. C., & Senay, M. C. 1995, AJ, 109, 1269
Flannery, B. P., & Ulrich, R. K. 1977, ApJ, 212, 533
Hastings, B., Langer, N., Wang, C., Schootemeijer, A., & Milone, A. P. 2021, A&A, 653, A144
Huang, W., Gies, D. R., & McSwain, M. V. 2010, ApJ, 722, 605
Kaitchuck, R. H. 1988, PASP, 100, 594
Kaitchuck, R. H. 1989, SSRv, 50, 51
Kaitchuck, R. H., & Honeycutt, R. K. 1982, ApJ, 258, 224
Kippenhahn, R., & Meyer-Hofmeister, E. 1977, A&A, 54, 539
Lubow, S. H., & Shu, F. H. 1975, ApJ, 198, 383
Maeder, A. 2003, A&A, 399, 263
Maeder, A., & Zahn, J.-P. 1998, A&A, 334, 1000
Mathis, S., Palacios, A., & Zahn, J.-P. 2004, A&A, 425, 243
Neo, S., Miyaji, S., Nomoto, K., & Sugimoto, D. 1977, PASJ, 29, 249
Packet, W. 1981, A&A, 102, 17
Paczyński, B. 1970, AcA, 20, 47
Paczyński, B. 1991, ApJ, 370, 597
Pols, O. R., Cote, J., Waters, L. B. F. M., & Heise, J. 1991, A&A, 241, 419
Popham, R., & Narayan, R. 1991, ApJ, 370, 604
Portegies Zwart, S. F. 1995, A&A, 269, 691
Porter, J. M., & Rivinius, T. 2003, PASP, 115, 1153
Raymer, E. 2012, MNRAS, 427, 1702
Richards, M. T. 1992, ApJ, 387, 329
Richards, M. T., Cocking, A. S., Fisher, J. G., & Conover, M. J. 2014, ApJ, 795, 160
Richards, M. T., & Ratliff, M. A. 1998, ApJ, 493, 326
Sana, H., de Mink, S. E., de Koter, A., et al. 2012, Sci, 337, 444
Shao, Y., & Li, X.-D. 2014, ApJ, 796, 37
Staritsin, E. 2021, A&A, 646, A90
Staritsin, E. 2022, RAA, 22, 105015
Staritsin, E. I. 1999, ARep, 43, 592
Staritsin, E. I. 2005, ARep, 49, 634
Staritsin, E. I. 2007, AstL, 33, 93
Staritsin, E. I. 2009, AstL, 35, 413S
Staritsin, E. I. 2014, ARep, 58, 808
Staritsin, E. I. 2019, Astrophysics and Space Science, 364, 110
Talon, S., & Zahn, J.-P. 1997, A&A, 317, 749
Tassoul, J.-L. 1978, Theory of Rotating Stars (Princeton, NJ: Princeton Univ. Press)
Van Bever, J., & Vanbeveren, D. 1997, A&A, 322, 116
Van Rensbergen, W., De Greve, J. P., Mennekens, N., Jansen, K., & De Loore, C. 2011, A&A, 528, A16
Zahn, J.-P. 1992, A&A, 265, 115